EQUINE VETERINARY JOURNAL
Equine vet. J. (2009) **41** (3) 285-291
doi: 10.2746/042516409X397136

Relationship between the forces acting on the horse's back and the movements of rider and horse while walking on a treadmill

K. VON PEINEN*, T. WIESTNER, S. BOGISCH, L. ROEPSTORFF†, P. R. VAN WEEREN‡ and M. A. WEISHAUPT

Equine Department, Vetsuisse Faculty University of Zurich, CH-8057 Zurich, Switzerland; †Department of Veterinary Anatomy and Physiology, Swedish University of Agricultural Sciences, 75007 Uppsala, Sweden; and ‡Department of Equine Sciences, Faculty of Veterinary Medicine, Utrecht University, Yalelaan 114, 3584 CM Utrecht, The Netherlands.

Keywords: horse; ground reaction forces; kinematics; rider; saddle force

Summary

Reasons for performing study: **The exact relationship between the saddle pressure pattern during one stride cycle and the movements of horse and rider at the walk are poorly understood and have never been investigated in detail.**

Hypothesis: **The movements of rider and horse account for the force distribution pattern under the saddle.**

Method: **Vertical ground reaction forces (GRF), kinematics of horse and rider as well as saddle forces (FS) were measured synchronously in 7 high level dressage horses while being ridden on an instrumented treadmill at walk. Discrete values of the total saddle forces (FStot) were determined for each stride and related to kinematics and GRF. The pressure sensitive mat was divided into halves and sixths to assess the force distribution over the horse's back in more detail. Differences were tested using a one sample *t* test ($P<0.05$).**

Results: **FStot of all the horses showed 3 peaks (P1–P3) and 3 minima (M1–M3) in each half-cycle, which were systematically related to the footfall sequence of the walk. Looking at the halves of the mat, force curves were 50% phase-shifted. The analysis of the FS of the 6 sections showed a clear association to the rider's and horse's movements.**

Conclusion: **The saddle force distribution during an entire stride cycle has a distinct pattern although the force fluctuations of the FStot are small. The forces in the front thirds were clearly related to the movement of the front limbs, those in the mid part to the lateral flexion of the horse's spine and the loading of the hind part was mainly influenced by the axial rotation and lateral bending of the back.**

Potential relevance: **These data can be used as a reference for comparing different types of saddle fit.**

Introduction

In many riding cultures, the saddle is the most important link between the rider and the horse. Because of its central role, saddle design must be optimised with regard for the horse's use, soundness and manoeuvrability. The assessment of saddle fit, formerly done empirically, depended upon the expertise of the assessing person and was confined to the static situation. Using pressure sensitive saddle mats, the influence of the saddle on the horses back can be studied while moving at different gaits. It has been shown that there is a weak association between the saddle pressures acting on the back in a standing horse and those exerted during movement (Jeffcott *et al*. 1999; Bojer *et al*. 2001). Pressure distribution was investigated for different saddle types (Harman 1994; Peham *et al*. 2004; Mönkemöller *et al*. 2005; Winkelmayr *et al*. 2006; Meschan *et al*. 2007), riding techniques (Peham *et al*. 2004; von Peinen *et al*. 2006; Geutjens *et al*. 2008) or muscle activity and mobility of the back (Peham and Schobesberger 2004). Saddle pressure measurements confirmed the association between clinical evidence of back pain and pressure peaks acting on the horse's back (Werner *et al*. 2002; Nyikos *et al*. 2005). Total saddle force curves show a characteristic, gait dependent pattern (Pullin *et al*. 1996; Jeffcott *et al*. 1999; Fruehwirth *et al*. 2004). However, the exact relationship to the movement of horse and rider, especially at walk, is still poorly understood.

In order to be able to construct well-fitting saddles it is essential to know how rider, saddle and horse interact and to explain the origin of the various saddle pressure peaks. In the present study this interrelationship was investigated for the different phases of a stride at walk.

Materials and methods

Horses, tack and riders

Seven clinically sound Warmblood dressage horses, one competing at intermediate and 6 at Grand Prix level, with mean (± s.d.) height at the withers of 1.70 ± 0.07 m and bwt of 609 ± 62 kg were investigated. All horses were accustomed to the treadmill (Mustang 2200)[1] and ridden by their own experienced rider (bwt 78 ± 17 kg) using their own fitted dressage saddle.

During the measurements the horses were ridden at walk at about 1.5 m/s with the neck raised, poll high and bridge of the nose slightly in front of the vertical. The correctness of execution was assessed by a qualified dressage judge (H.M.).

*Author to whom correspondence should be addressed.
[Paper received for publication 11.06.08; Accepted 29.10.08]

Data acquisition

Vertical ground reaction forces (GRF), of all 4 limbs (LF, RF, LH, RH) were simultaneously recorded with the treadmill integrated force measuring system (TiF, Weishaupt *et al*. 2002). From the GRF data, temporal data for stride duration, stride frequency and individual limb contact times (time of first contact, time of toe-off) were determined using custom made software (HP2)[2].

Saddle pressures were measured with a Pliance-X System[3]. The pressure sensitive mat consisted of 2 separate parts each with 128 sensors in a 16 x 8 (longitudinal x transverse) array. Every sensor had a size of 4.7 x 3.1 cm (14.57 cm²). The 2 mat parts were placed symmetrically on each side of the horse's back. Zero baseline was established before saddling and tightening the girth. For the kinematic measurements, spherical reflective markers (diameter 19 mm) were placed over the following anatomic landmarks of horse and rider and on the saddle: 1) *horse*: on the cranial end of the wing of atlas on the left side, on the spinous processes of T6, L3, S3, on the scapulae at mid point between the *pars tuber spinae scapulae* and the shoulder joint on both sides, on the left and right *tuber coxae* and on the lateral hoof walls of the left front and hind hoof at the height of the coffin joint; 2) *rider*: on the sacrum and over the left and right hip joint; and 3) *saddle*: on the left and right buttons at the pommel and on both sides at the caudal ends of the panels.

Qualisys Track Manager software[4] was used to track the markers recorded by 12 ProReflex infrared cameras[4]. Further details are described elsewhere (Gómez Álvarez *et al*. 2006; Rhodin 2008). The right-handed coordinate system was aligned with the treadmill; the x-axis in direction of the horse's head and the z-axis pointing upwards.

Synchronised records of 10 s were made with the 3 measuring systems. Depending on the viewing quality of the markers for the ProReflex cameras, a frame rate of 140 Hz or 240 Hz was chosen; accordingly, integer rates of sampling frequencies for the Pliance-X system (70Hz, 60Hz) and the TiF system (420Hz, 480 Hz) were used.

Data analysis and statistics

All data strings and the limb contact times from TiF were imported into MatLab[5] for further analysis. Based on the stride-cycle times of the left forelimb, records were split into strides, time-normalised to 101 points (0–100% stride) and averaged to mean stride values. GRF data were normalised to the combined weight of horse and rider (% hrwt). Saddle pressure data were converted to saddle force (FS) values and normalised to the rider's weight (% rwt), which included the weight of the saddle and instrumentation. The weights were determined from the force data intrinsically: Theoretically, the mean vertical force (F_{mean}) acting on a body mass (m) over a complete stride cycle is $F_{mean} = m\ \boldsymbol{g}$. Thus, the weight used for normalisation (hrwt, rwt) was the overall mean of total GRF or total FS, respectively, determined from all strides of a record. FS of the entire mat (FStot), of the left (FSL) and the right (FSR) halves of the mat were calculated. Additionally, the saddle mat halves were divided into 3 transverse sectors. Each sector occupied 1/3 of the longitudinal extent of the actually loaded sensor area. A FS curve for each of the 6 sectors was determined. All stride normalised force and kinematic data were expressed as the deviation from the respective stride mean and a group mean curve was calculated for illustration.

Discrete values were determined from all the stride normalised FS curves of each horse separately: 1) the stride mean, representing the mean weight distribution onto the sectors; 2) the magnitude of the local maxima (P1, P2, P3) and local minima (M1, M2, M3), expressed as the deviation from the respective stride mean; and 3) the time of the respective maxima and minima.

Time points within the first half stride referred to first contact of FL whereas the time points of the second half stride referred to first contact of FR. Since the walk is a symmetrical gait both half cycles are mirror imaged. This allowed the pooling of corresponding amplitude and time values.

The times (% stride) of all FS extremes were related to GRF stance time events and/or characteristic events of the kinematic data. All discrete values in this study are pooled values.

Time coincidences of the extremes with different stride normalised parameters or the footfall beat times, were assessed with paired *t* tests. Amplitude deviations from the respective mean

TABLE 1: Mean (± s.d.) of total saddle force (FStot), kinematic and ground reaction force parameter/events as they occur in the 4 phases of the first half-cycle of the stride (n = 7 ridden horses at walk)

Parameter/event	Extremes	Time % stride
Phase 1		
First contact FL		0.0 ± 0.0
M1		2.9 ± 1.7
z-amplitude: T6	min	4.9 ± 1.9
P1		10.0 ± 2.3
z-amplitude: S3	max	10.9 ± 1.7 **a**
z-distance: rider sacrum - saddle hind	min	11.2 ± 1.2 **a**
x-rotation: rider hip	max	11.3 ± 2.5 **a**
Phase 2		
Toe off RF		13.5 ± 1.3
GRF tot	min	14.1 ± 1.4 **b**
x-distance: saddle front - T6	min	17.0 ± 3.6 **a**
M2		18.6 ± 3.8
back: dorsoventral flexion	max	21.5 ± 4.2
x-rotation: shoulder	max	22.6 ± 1.0
z-rotation: saddle hind	max	22.6 ± 2.8
P2		26.7 ± 1.7 **b**
Phase 3		
First contact RH		26.8 ± 2.5
x-distance: saddle hind - rider's sacrum	max	27.2 ± 3.0
x-rotation: saddle hind	max	28.9 ± 1.5 **c**
Back: lateral bending	max	29.9 ± 2.3 **c**
z-amplitude: atlas	min	32.5 ± 3.1 **a**
z-rotation: hip	min	33.2 ± 4.3 **a**
GRF tot	max	33.7 ± 2.8 **a**
z-amplitude: S3	min	33.9 ± 2.0 **a**
M3		34.4 ± 2.6
z-amplitude: T6	max	35.1 ± 3.2 **a**
x-distance: saddle front - T6	max	35.2 ± 1.8 **b**
z-distance: rider sacrum - saddle hind	max	35.2 ± 2.3 **a**
Back: dorsoventral flexion	min	41.0 ± 3.7 **b**
Phase 4		
Toe off LH		41.4 ± 2.4
P3		44.0 ± 3.2
x-rotation: hip	max	46.0 ± 1.4 **a**
Protraction hoof FR	max	46.6 ± 1.0 **a**
First contact RF		49.9 ± 1.2

The time of extremes of FStot are given in bold. If not mentioned differently, the results relate to the movement of the horse. Abbreviations: LF, left front; RF, right front; LH, left hind; RH, right hind. GRF tot: sum of the ground reaction forces of all 4 limbs. T6, S3: Spinous processes of T6 and S3, respectively. Rotation: rotation around the indicated axis (for sign see legend of Figure 4). Results of the paired t-test: **a**: time of event coincides with (i.e. could not be statistically differentiated from) FStot extremes: **b**: time of event coincides with toe off or first contact time of a limb; **c**: events that coincide with each other.

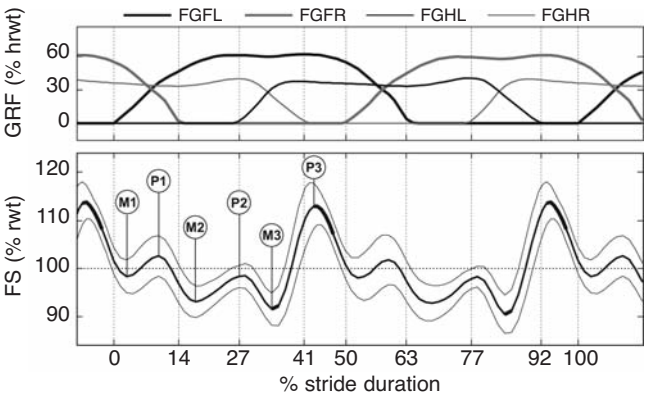

Fig 1: Mean stride normalised ground reaction forces (top) and total saddle force (bottom) of 7 horses at walk. Ground reactions forces of individual limbs (FG limb) are expressed as percentage of the total weight of horse and rider (% hrwt). Total saddle force (FS) is expressed as percentage of the rider's weight (% rwt). Thin lines indicate ± s.e.; bold curve sections mark significant deviations from rider weight (P<0.05). The local extremes (minima M1 to M3, maxima P1 to P3) are indicated. The abscissa is scaled in % of stride; the vertical grid lines indicate the mean first contact and toe off times dividing the stride into 8 support phases.

of the entire stride were tested with one group *t* tests. Type I error $\alpha = 0.05$ was used to test for significance.

The experimental protocol was approved by the Animal Health and Welfare Commission of the canton of Zurich, Switzerland.

Results

The 7 horses moved at a mean ± s.d. speed of 1.46 ± 0.01 m/s, had a stride frequency of 50.9 ± 1.7 strides/min and a stride duration of 1.180 ± 0.041 s. Walking horses show 8 distinct support phases (Fig 1, Clayton 2004), which are defined by the first contact and toe-off times of each of the 4 limbs (Table 1). Since the walk is a symmetrical gait, the subsequent description is given for the left half cycle only, i.e. *Phase 1* to *Phase 4*.

On the FStot curves of all horses 3 local minima (M1–M3) and 3 local maxima (P1–P3) for each half-cycle could be identified. The extremes could be assigned systematically to one of the 4 phases: M1 and P1 to *Phase 1*, M2 to *Phase 2*, P2 coincided with the end of *Phase 2* (first contact of the right hindlimb), M3 to *Phase 3* and P3 to *Phase 4* (Fig 1). Values of extremes are listed in Table 2. Comparing the force curves of the left and the right mat halves as well as the corresponding left and right thirds almost identical curves were observed, albeit shifted in time by a half-cycle (Fig 2).

The force distributions in the 6 sections of the saddle mat at the time points of the extremes of FStot are listed as discrete values in Table 2 and illustrated in Figure 3. Selected kinematic parameters are shown in Figure 4 and events that directly coincide with FStot extremes are listed in Table 1.

Mean ± s.d. saddle force of the entire stride was 31 ± 7% rwt in the frontal thirds (FSLf + FSRf), 38 ± 3% rwt in the central thirds (FSLc + FSRc) and 31 ± 6 % rwt in the hind thirds (FSLh + FSRh). The difference between the centre and front was significant (P<0.05) (Table 2).

Phase 1

At the moment of M1 during the first tripedal support phase (2 fore-, one hindlimb), the withers were at their lowest point and the croup was moving upwards. Only FSLf and FSRf of the mat showed a deviation from the average weight; on the left side a positive, on the right side a negative value. P1 occurred approximately 6% of stride duration later than M1. The croup was now at its highest point and the rider sat deepest into the saddle (Table 1). Viewed from behind his pelvis started to tilt to the right, together with the horse's back which flexed to the right. The hind left part of the saddle moved away from the horse's spine (Fig 3). The peak in the FStot was not very distinct since the positive amplitude of FSLf was cancelled out by the negative value of FSLh (Fig 2).

Phase 2

During the left lateral support phase the back reached its maximal dorsoflexion. The x-distance between T6 and the front part of the saddle was minimal (Table 1). The rider was at the most forward in the saddle and was in upward motion. The negative value of FSLh and FSRc resulted in M2 of the total force curve.

The following event (P2) coincided with the end of *Phase 2* (Table 1). While FSLh still remained negative, FSLc showed a clear positive peak.

Phase 3

In *Phase 3* the back reached its maximal lateroflexion which coincided with the maximal rotation of the saddle around the x-axis to the right (Fig 3). The rider's lift out of the saddle was at its greatest. The withers were at the highest and the croup at the lowest point, resulting in maximal back inclination (Fig 4). The x-distance between the front part of the saddle and withers was maximal (Table 1). The sum of the saddle forces of the 6 parts resulted in the most distinct minimum (M3), mainly caused by the frontal thirds (Fig 2).

TABLE 2: Saddle force distribution within the 6 mat sections. Mean force for the total stride in each sector (column 2) and deviation from the stride mean, determined for the time points of FStot extremes M1 to P3

Mat sector	Total stride mean % rwt	**M1** Δ % rwt	**P1** Δ % rwt	**M2** Δ % rwt	**P2** Δ % rwt	**M3** Δ % rwt	**P3** Δ % rwt
FStot	100	-3.7 ± 11.7	4.2 ± 11.9	-8.8 ± 7.8 **a**	0.8 ± 7.4	-11.4 ± 9.3 **a**	17.3 ± 10.6 **a**
FSLf	16.1 ± 3.3	4.1 ± 2.2 **a**	4.5 ± 3.2 **a**	-0.7 ± 1.6	-1.1 ± 2.3	-4.5 ± 2.3 **a**	-2.6 ± 0.9 **a**
FSLc	19.4 ± 1.8	-0.3 ± 1.5	0.5 ± 1.9	-1.6 ± 2.1	3.7 ± 2.2 **a**	1.3 ± 1.3 **a**	2.7 ± 1.4 **a**
FSLh	15.7 ± 3.7	-0.2 ± 1.8	-2.1 ± 0.8 **a**	-3.0 ± 1.7 **a**	-3.1 ± 2.8 **a**	-4.8 ± 3.0 **a**	-0.4 ± 2.3
FSRf	15.0 ± 4.1	-4.0 ± 2.6 **a**	1.1 ± 3.4	0.9 ± 3.0	-0.6 ± 1.3	-4.4 ± 1.1 **a**	4.8 ± 2.5 **a**
FSRc	18.5 ± 2.2	-1.6 ± 2.8	-0.2 ± 2.2	-3.7 ± 1.8 **a**	-1.1 ± 1.4	-1.4 ± 2.2	3.9 ± 5.2
FSRh	15.2 ± 3.3	-1.1 ± 4.1	0.8 ± 3.3	-1.0 ± 2.5	2.4 ± 2.3 **a**	2.6 ± 4.2	8.8 ± 6.3 **a**

Data are given as mean ± s.d. (7 horses) expressed as percentage of rider weight (% rwt). Forces of the total mat (FStot); left frontal (FSLf), central (FSLc), hind (FSLh) section of the mat and correspondingly for the right side (FSRf, FSRc, FSRh). **a**: Significant differences (P<0.05) from total stride mean of the respective sector.

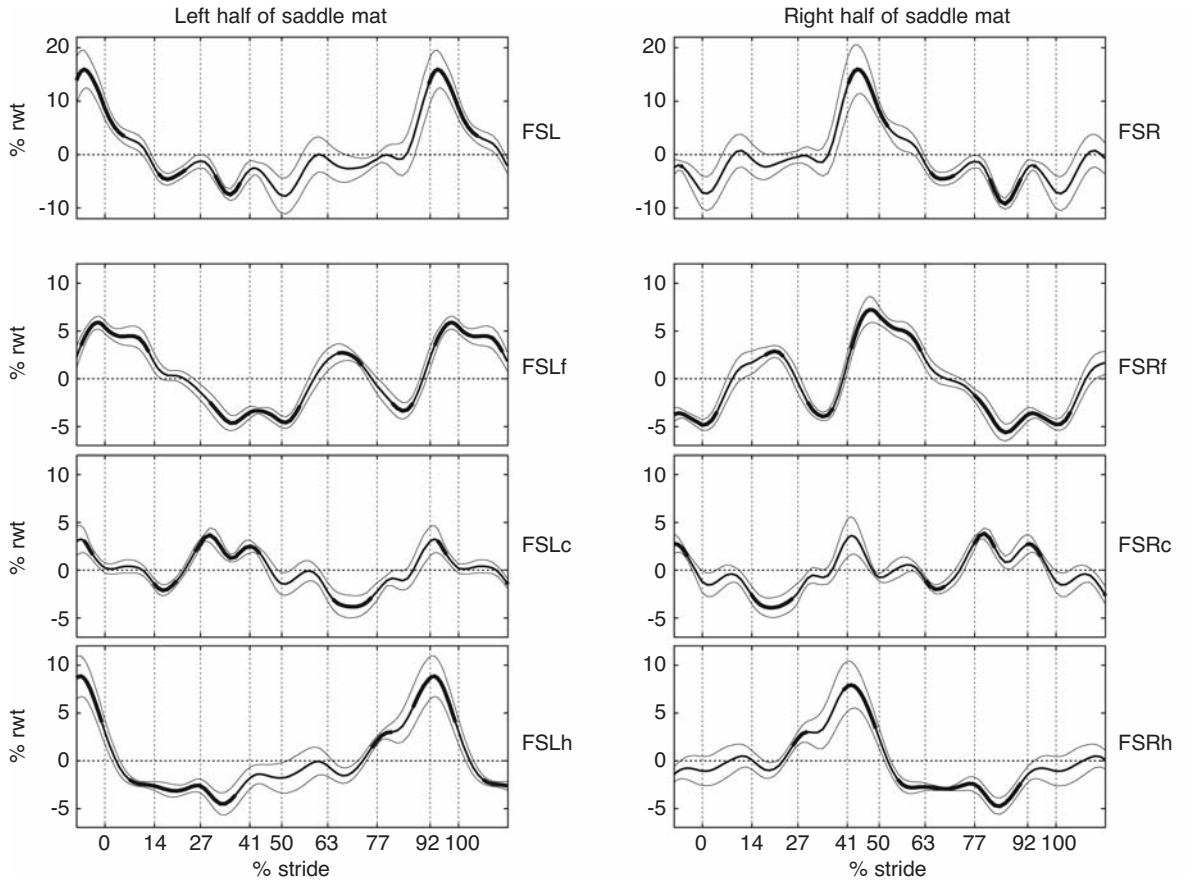

Fig 2: Mean (± s.e.) stride normalised saddle forces of the left (FSL) and right (FSR) mat half and partial forces of 6 sectors of 7 horses. Each mat half was divided into a frontal (f), central (c) and hind (h) sector; partial forces were labelled accordingly. Bold curve sections mark significant deviations from the stride mean of the respective sector (P<0.05). For scaling of the abscissa see Figure 1.

Phase 4

At the beginning of *Phase 4* the toe-off event of the left hindlimb led to an abrupt anticlockwise rotation of the pelvis around the x-axis (Fig 3). At the point where the hip was rotated maximally, the right forelimb was in maximal protraction and rider and horse were in a counteracting movement, i.e. the rider was moving downwards and the horse's croup upwards the most prominent force peak (P3) occurred, mainly caused by the right front and hind third (FSRf, FSRh; Fig 2).

Discussion

As shown previously (Fruehwirth *et al*. 2004), the total saddle force curve at the walk has a characteristic shape. In the present study, 3 and not only 2 peaks per half-stride were observed; however, the most distinct peak (P3) also occurred approximately halfway through the stride cycle (50% of stride) (Fig 1). This difference could be due to the fact that the horses were walking on a treadmill at constant speed and on a homogeneous and even surface whereas in the former study they were ridden on a pressed sand track at undefined velocities. Treadmill locomotion, as well as different ground surfaces change the horse's movement pattern in a subtle way (Buchner *et al*. 1994). Whether the different conditions are the reason for the variation of the FStot curve, remains unknown.

The division of the pressure mat into 6 parts gave a closer insight into the origin of the saddle force peaks. Saddle fitting problems, such as bridging or pinching at the withers, are mainly evident in the front and hind part of the saddle area (Harman 2004). Using a similar subdivision of the mat, corresponding phenomena could be detected by other investigators (Werner *et al*. 2002; Mönkemöller *et al*. 2005; Nyikos *et al*. 2005).

Besides the vertical movement of the rider, the components of the saddle force could mainly be associated with the movement of the forelimbs, the lateral flexion and unilateral contraction of the horse's back muscles as well as with the rotation of the horse's pelvis.

Vertical movement of horse and rider

The walk is a gait without suspension phase and with a rocking type of movement; when the withers move upwards, the croup moves down and *vice versa*. The closest contact of the rider to the saddle (Fig 4) occurred at P1 of the FStot, which coincided with the time where the S3 marker was the highest (Table 1) and the back inclination minimal (Fig 4). Contrary to expectations, the deceleration of the rider at this moment is hardly reflected in the saddle forces; it only produces a small positive impulse in the FSLf curve (Fig 2), which produced a nonsignificant component in the FStot curve (Fig 1). The largest dissociation of rider and saddle coincided with M3 of the total FS. At this moment, a force deficit is clearly evident in both frontal mat sectors (Fig 2), which corresponds to the prominent M3 and is significantly lower than the mean rider weight (Fig 1). Because there is no plausible explanation for P3 regarding to the vertical movement of horse and rider, it must be concluded that some FS components are of

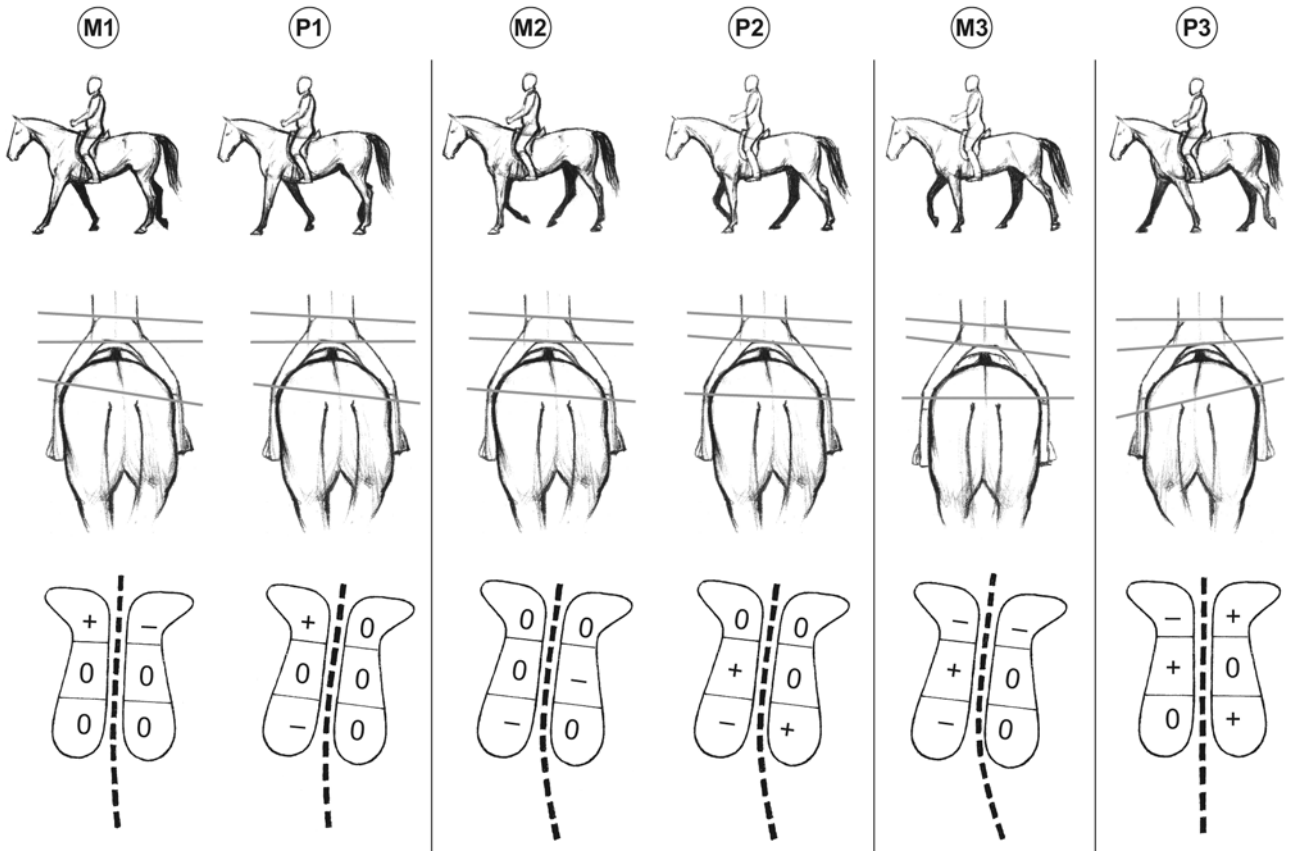

Fig 3: Footing sequence (top), x-rotation angles of rider, saddle and horse's hip (middle) as well as saddle mat force changes and lateroflexion of the back (bottom) at the time points where the total saddle force reached one of the defined local minima (M1–M3) or maxima (P1–P3). Rotation angles are approximately 2-fold enlarged in order to illustrate the differences for the various time points. The back curvature is only qualitative. For the 6 saddle mat sectors, positive (+), negative (-) and no (0) deviation from the sector's stride mean are indicated based on values in Table 2.

different origin. This observation contrasts with the situation in the trot, where the saddle force extremes are mainly caused by the vertical movement of the rider (von Peinen *et al*. 2006).

Forelimb movement

The force components in the front third of the mat in particular were closely related to the movement of the front limbs. Some of the muscles (*M. trapezius pars caudalis*, *M. spinalis*), which are responsible for the retraction of the proximal part of the scapula and the elevation of the neck, are located beneath the front part of the saddle. This part of the saddle's construction is very rigid due to the headplate. During forelimb protraction the proximal end of the scapula moves backwards, and the head and neck are in upward motion. The *trapezius* and *spinalis* muscles are functionally active. Concurrently, the contralateral forelimb is retracted with the proximal end of the scapula fully forward and the *trapezius* muscle relaxed and stretched. It is assumed that this difference in muscle diameter and tension results in an uneven resistance underneath the headplate and therefore, to an asymmetric force distribution in the front part of the saddle area. Unilateral muscle activation during forelimb protraction was recorded by surface EMG in the area of T12 by Licka *et al*. (2008).

Lateroflexion

In the central part of the saddle, the lateral flexion of the horse's back was probably mainly responsible for the force variation. In *Phase 3* the spine was flexed maximally to the right with a concurrent contraction of the *M. longissimus dorsi* at the convex side. Licka *et al*. (2008) measured increased EMG activity of the *longissimus dorsi* muscles at T16 on the side where the hindlimb was about to push off. The muscle activity on the ipsilateral side is needed to counteract the lateroflexion of the spine due to the rotation of the pelvis generated by the propulsive forces of the hindlimb. Therefore, it can be concluded that the higher muscular tonus increases resistance to the saddle panel on the convex side of the back. Additionally, the lateroflexion of the horses back towards the left panel increasing the FSLc. This clarifies why a narrow gullet could potentially limit the lateral movements of the spine (Harman 2004).

Pelvic rotation

Between mid *Phase 3* to mid *Phase 4* the most prominent event in the hindquarters occurred. The toe-off of the left hindlimb led to an abrupt and maximal anticlockwise rotation of the pelvis around the x-axis (Fig 3) causing the distinct force peak in the FSRh.

Conclusion

At walk, the saddle forces reflect the vertical movement of horse and rider to a lesser extent then at the trot. It could be shown that the horse's muscular activity, the lateral flexion and axial rotation were the main causes for the shape of the FStot curve with the

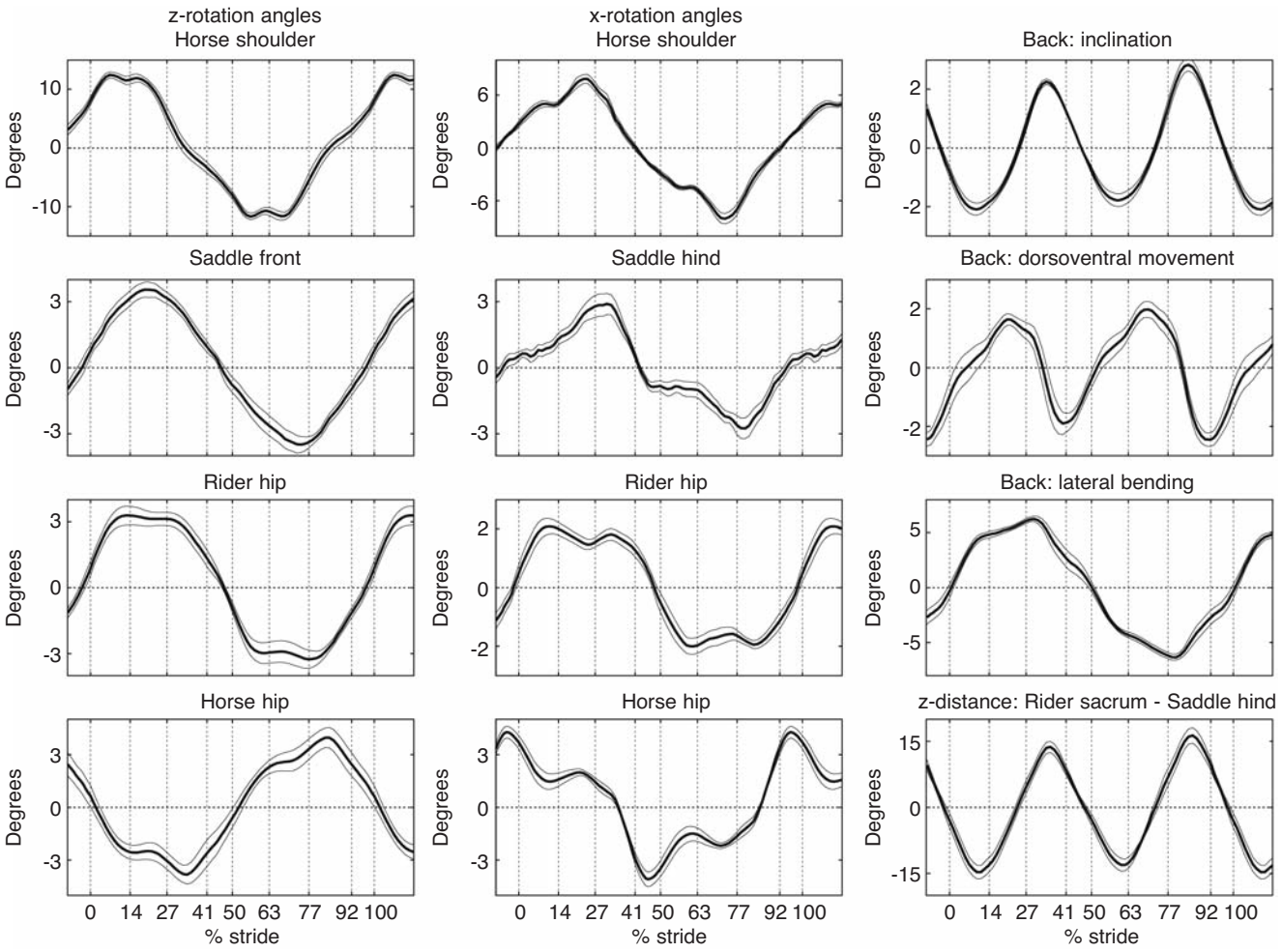

Fig 4: Selected mean (± s.e.) stride normalised kinematic parameters for rotation and distance for all 7 horses. The rotation angles refer to the axis indicated and are positive for clockwise rotation if horses are seen from behind (x-rotation) and from above (z-rotation). Back, inclination: angle of inclination compared to the front of the horse; positive when T6 higher than S3. Back, dorsoventral movement: angle T6–L3–S3, projected onto XZ-plane (vertical), positive angle if more flexed. Back, lateral bending: lateral flexion angle T6–L3–S3, projected onto XY-plane (horizontal), positive angles for bending to the right. For scaling of the abscissa see Figure 1.

2 extremes M3 and P3. Special attention has to be directed to the following aspects when choosing a saddle: 1) the width of the headplate, which might limit the movement of the forehand; 2) the wideness of the gullet, which should allow the lateral bending of the spinal column; and 3) the shape and stuffing of the panels in the mid and hind part of the saddle, which should ensure unhindered movement of the lumbar back and the hindquarters.

All these factors may negatively influence the suppleness of the back. To clarify these findings and define the maximally tolerated forces under the saddle at the different locations, further investigations are needed.

Acknowledgements

This study was supported by a grant of the 'Stiftung Forschung für das Pferd'. The authors wish to thank all riders and horse owners who kindly lent us their horses for this study, Heinz Meyer for his contribution of dressage knowledge and for professionally judging the riders and horses throughout all the trials, as well as Marie Rhodin, Constanza Gómez-Álvarez, Anna Byström and Nina Waldern for excellent technical assistance and Isabel Imboden for English corrections.

Manufacturers' addresses

[1]Kagra AG, Fahrwangen, Switzerland.
[2]University of Zurich, Zurich, Switzerland.
[3]Pliance, Novel GmbH, Munich, Germany.
[4]Qualysis, Gothenburg, Sweden.
[5]The Math Works Inc., Natick, Massachusetts, USA.

References

Bojer, M., Brüggemann, G., Kersting, U. and Lötzerich, H. (2001) Vergleichende Untersuchung von elektronischen Satteldruckmessungen beim Pferd im Stand und in der Bewegung, Deutsche Sporthochschule, Köln.

Buchner, H.H.F., Savelberg, H.H.C.M., Schamhardt, H.C., Merkens, H.W. and Barneveld, A. (1994) Kinematics of treadmill versus overground locomotion in horses. *Vet. Quart.* **16**, S87-S90.

Clayton, H.M. (2004) The gaits. In: *The Dynamic Horse*, Sport Horse Publications, Manson, Michigan. p 171.

Fruehwirth, B., Peham, C., Scheidl, M. and Schobesberger, H. (2004) Evaluation of pressure distribution under an English saddle at walk, trot and canter. *Equine vet. J.* **36**, 754-757.

Geutjens, C.A., Clayton, H.M. and Kaiser, L.J. (2008) Forces and pressures beneath the saddle during mounting from the ground and from a raised mounting platform. *Vet. J.* **175**, 332-337.

Gómez Álvarez, C.B., Rhodin, M., Bobber, M.F., Meyer, H., Weishaupt, M.A., Johnston, C. and van Weeren, P.R. (2006) The effect of head and neck position on

the thoracolumbar kinematics in the unridden horse. *Equine vet. J., Suppl.* **36**, 445-451.

Harman, J.C. (1994) Practical use of a computerized saddle pressure measuring device to determine the effects of saddle pads on the horses back. *J. equine vet. Sci.* **14**, 606-611.

Harman, J. (2004) Saddle fit on the horse. In: *The Horse's Pain-free Back and Saddle-Fit Book*, Kenilworth Press, Buckingham. pp 51-82.

Jeffcott, L.B., Holmes, M.A. and Townsend, H.G. (1999) Validity of saddle pressure measurements using force-sensing array technology - preliminary studies. *Vet. J.* **158**, 113-119.

Licka, T., Frey, A. and Peham, C. (2008) Electromyographic activity of the longissimus dorsi muscles in horses when walking on a treadmill. *Vet. J.* doi:10.1016/j.tvjl.2007.11.001

Meschan, E.M., Peham, C., Schobesberger, H. and Licka, T.F. (2007) The influence of the width of the saddle tree on the forces and the pressure distribution under the saddle. *Vet. J.* **173**, 578-584.

Mönkemöller, S., Keel, R., Müller, J., Kalpen, A., Geuder, M., Auer, J.A. and von Rechenberg, B. (2005) PLIANCE MOBILE-16HE: Eine Folgestudie über elektronische Satteldruckmessung nach Anpassung der Sattelsituation. *Pferdeheilkunde* **21**, 102-114.

Nyikos, S., Werner, D., Müller, J.A., Buess, C., Keel, R., Kalpen, A., Vontobel, H.D., von Plocki, K.A., Auer, J.A. and von Rechenberg, B. (2005) Measurements of saddle pressure in conjunction with back problems in horses. *Pferdeheilkunde* **21**, 187-198.

Peham, C. and Schobesberger, H. (2004) Influence of the load of a rider or of a region with increased stiffness on the equine back: a modelling study. *Equine vet. J.* **36**, 703-705.

Peham, C., Licka, T., Schobesberger, H. and Meschan, E. (2004) Influence of the rider on the variability of the equine gait. *Hum. Mov. Sci.* **23**, 663-671.

Pullin, J.G., Collier, M.A., Durham, C.M. and Miller, R.K. (1996) Use of force sensing array technology in the development of a new equine saddle pad: Static and dynamic evaluations and technical considerations. *J. equine vet. Sci.* **16**, 207-216.

Rhodin, M. (2008) *A Biomechanical Analysis of Relationship between the Head and Neck Position, Vertebral Column and Limbs in the Horse at Walk and Trot,* Doctoral Thesis, Swedish University of Agricultural Sciences, Uppsala.

Von Peinen, K., Wiestner, T., Keel, R., Roepstorff, L., Meyer, H., van Weeren, R. and Weishaupt, M.A. (2006) Saddle force measurements in relation to ground reaction forces in different head neck positions in the ridden horse. In: *Proceedings of the 7th International Conference of Equine Exercise Physiology*, ICEEP Publications. p 124.

Weishaupt, M.A., Hogg, H.P., Wiestner, T., Denoth, J., Stüssi, E. and Auer, J.A. (2002) Instrumented treadmill for measuring vertical ground reaction forces in horses. *Am. J. vet. Res.* **63**, 520-527.

Werner, D., Nyikos, S., Kalpen, A., Geuder, M., Haas, C., Vontobel, H.D., Auer, J.A. and von Rechenberg, B. (2002) Druckmessungen unter dem Sattel: eine Studie mit einem elektronischen Sattel-Messsystem (Novel GmbH). *Pferdeheilkunde* **18**, 124-140.

Winkelmayr, B., Peham, C., Fruehwirth, B., Licka, T. and Scheidl, M. (2006) Evaluation of the force acting on the back of the horse with an English saddle and a side saddle at walk, trot and canter. *Equine vet. J., Suppl.* **36**, 406-410.

Author contributions The initiation, conception and planning for this study were by K.v.P., T.W., L.R., P.R.v.W. and M.A.W. Its execution was by K.v.P., T.W., L.R. and M.A.W., with statistics by K.v.P., S.B. and L.R., and the paper was written by K.v.P., S.B., T.W. and M.A.W.